MOLECULAR AND CELLULAR BIOLOGY, Aug. 2001, p. 5321–5331 Vol. 21, No. 16
0270-7306/01/$04.00+0 DOI: 10.1128/MCB.21.16.5321–5331.2001

Mice with Very Low Expression of the Vesicular Monoamine Transporter 2 Gene Survive into Adulthood: Potential Mouse Model for Parkinsonism

KATRIN A. MOOSLEHNER,[1]* POK MAN CHAN,[1,2] WEIMING XU,[3] LIZHI LIU,[3] CLAIRE SMADJA,[1]†
TREVOR HUMBY,[1] NICHOLAS D. ALLEN,[1] LAWRENCE S. WILKINSON,[1] AND PIERS C. EMSON[1]

The Babraham Institute, Neurobiology Programme, Babraham, Cambridge CB2 4AT,[1] Department of Zoology, University of Cambridge, Cambridge CB2 3EJ,[2] and The Rayne Institute, University College London, London WCIE 6JJ,[3] United Kingdom

Received 13 March 2001/Accepted 8 May 2001

We have created a transgenic mouse with a hypomorphic allele of the vesicular monoamine transporter 2 (*Vmat2*) gene by gene targeting. These mice (KA1) have profound changes in monoamine metabolism and function and survive into adulthood. Specifically, these animals express very low levels of VMAT2, an endogenous protein which sequesters monoamines intracellularly into vesicles, a process that, in addition to being important in normal transmission, may also act to keep intracellular levels of the monoamine neurotransmitters below potentially toxic thresholds. Homozygous mice show large reductions in brain tissue monoamines, motor impairments, enhanced sensitivity to dopamine agonism, and changes in the chemical neuroanatomy of the striatum that are consistent with alterations in the balance of the striatonigral (direct) and striatopallidal (indirect) pathways. The VMAT2-deficient KA1 mice are also more vulnerable to the neurotoxic effects of 1-methyl-4-phenyl-1,2,3,6-tetrahydropyridine in terms of nigral dopamine cell death. We suggest that the mice may be of value in examining, long term, the insidious damaging consequences of abnormal intracellular handling of monoamines. On the basis of our current findings, the mice are likely to prove of immediate interest to aspects of the symptomatology of parkinsonism. They may also, however, be of use in probing other aspects of monoaminergic function and dysfunction in the brain, the latter making important contributions to the pathogenesis of schizophrenia and addiction.

There are three major monoaminergic cell groups, ramifying extensively throughout the brain and distinguished by their neurotransmitter phenotype: noradrenaline (norepinephrine), dopamine, and serotonin (3, 5, 25). The neural specific vesicular monoamine transporter 2 (VMAT2) packages these monoamine neurotransmitters into vesicles after they have been synthesized from their amino acid precursors, tyrosine and tryptophan, in the nerve terminal. This sequestering action is important for normal neurotransmission and may also act to keep intracellular levels of the monoamine transmitters below potentially toxic levels (7, 19). The diffuse monoamine systems modulate a wide range of brain functions, spanning sensorymotor, motivational, and cognitive domains. Abnormalities in the functioning of these systems have been suggested to play key roles in the etiology of a number of disorders, including Parkinson's disease (4), schizophrenia (6, 32), and addiction (16, 26).

We have created a transgenic mouse by utilizing a targeted insertion in which endogenous VMAT2 is no longer expressed at levels detectable by in situ hybridization and immunohistochemistry methods and in which there are major changes in monoamine metabolism. Unlike other reported knockouts of the *Vmat2* gene (9, 34, 36), these mice survive into adulthood as homozygotes and do not suffer gross physical defects, offering a unique opportunity to examine more subtle aspects of the behavioral and brain phenotypes resulting from abnormal intracellular handling of monoamine transmitters. Here we report on the creation of the mouse and provide data at the behavioral, neurochemical, and molecular levels which recapitulate some of the symptomatology of Parkinson's disease and which may therefore provide insight into possible neuropathological mechanisms contributing to this neurodegenerating condition.

MATERIALS AND METHODS

Targeting vector construction. The mouse *VMAT2* locus was cloned from a partial *Mbo*I 129/Sv genomic library. Genomic *Sac*I and *Hin*dIII subclones were generated in pBluescript (Stratagene). The β-actin *neo* cassette (kindly supplied by Austin Smith, Centre for Genome Research, Edinburgh, United Kingdom) was cloned into the *Bam*HI site of a 2.5-kb *Hin*dIII-*Bam*HI fragment containing the *Vmat2* promoter and the leader exon in pBluescript (Stratagene). A 2.2-kb *Pvu*II fragment from the third intron of the *Vmat2* gene was cloned into the blunt-ended *Not*I site of this construct. The herpes simplex virus thymidine kinase gene (21) used for negative selection was cloned into the *Bg*III site at the 3′ end of the construct. The structure of the targeting vector is shown in Fig. 1A.

Gene targeting in ES cells. The targeting vector (30 μg) was linearized with *Sal*I and introduced into 129/Ola CGR 8.8 embryonic stem (ES) cells (1×10^7 cells; kindly supplied by William Scarnes, Centre for Genome Research) by electroporation. Transfected cells were seeded onto Neo^r STO feeder cells, and double selection (150 μg of G418/ml, 2 μM ganciclovir) was started 24 h after electroporation. A total of 325 double-drug-resistant colonies were picked 8 to 11 days after electroporation and screened for homologous recombination by Southern blot analysis. Six clones were identified as being correctly targeted with the 3′ external probe. Using a 5′ external probe, we found that in five out of those six clones homologous recombination resulted in the deletion of exons 1 and 2 (see Fig. 3B), resulting in a *Vmat2* null allele. Homozygous mice derived from one of these cell lines (GB1/1) died shortly after birth. In the KA1 cell line, one

* Corresponding author. Mailing address: Laboratories of Molecular and Cognitive Neuroscience, The Babraham Institute, Cambridge CB2 4AT, United Kingdom. Phone: 44-1223-496502. Fax: 44-1223-496022. E-mail: katrin.mooslehner@bbsrc.ac.uk.

† Present address: The Laboratory of Neuropharmacology, JE MESR 92-372, Faculte de Pharmacie, Châtenay-Malabry, France.

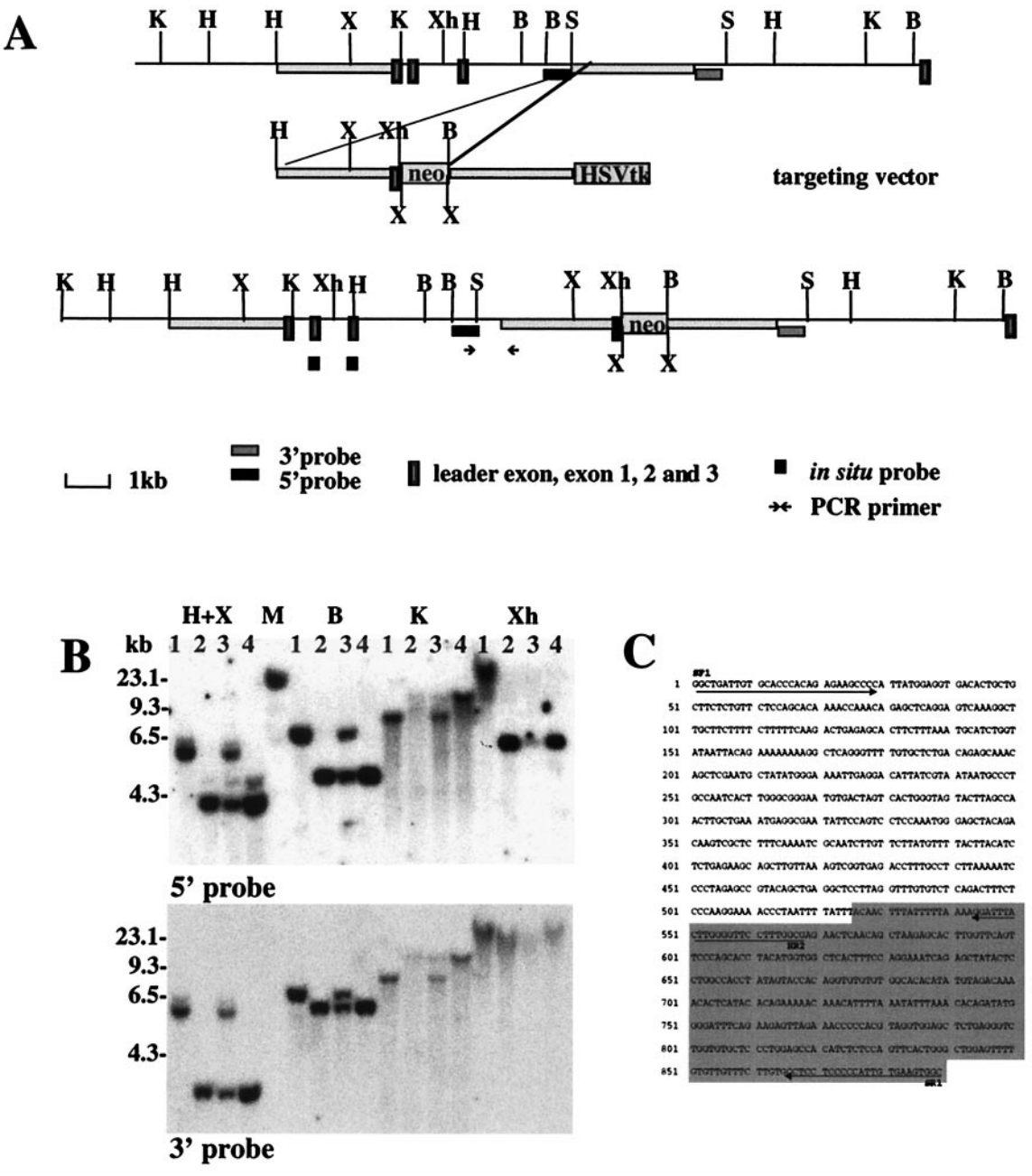

FIG. 1. Targeted insertion into the third intron of the *Vmat2* gene. (A) The *Vmat2* gene in the 129 wild-type mouse genome and mutant sequences after targeted insertion of the vector, with prominent restriction endonuclease sites shown (B, *Bam*HI; H, *Hin*dIII; K, *Kpn*I; S, *Sac*I; X, *Xba*I; and Xh, *Xho*I). Neomycin resistance sequences (neo) and sequences recognized by the *Vmat2* 3′ and 5′ hybridization probes are indicated. Homologous sequences in the mouse genome and of the targeting vector and the neomycin resistance (neo) and the herpes simplex virus thymidine kinase (HSV tk) sequences are indicated. (B) Southern blot analysis of hybridization of radiolabeled *Vmat2* 5′ and 3′ hybridization probes with genomic DNA extracted from the tail tips of wild-type (lane 1), heterozygous (lane 3), and homozygous (lanes 2 and 4) mice digested with the restriction endonucleases *Hin*dIII and *Xba*I (H+X), *Bam*HI (B), *Kpn*I (K), or Xhol (Xh). (C) Sequence of the PCR product generated with a forward primer specific for the 5′ flanking genomic sequences (SF1) and a reverse primer specific for the 5′ end of the transgene (SR1) (see also PCR primer in panel A). (D) *Vmat2* RNA expression in the major monoaminergic cell body groups in the brain of homozygous KA1 mice. In situ hybridization was carried out using end-labeled radioactive oligonucleotides complementary to the first and second exon of the *Vmat2* gene (see also panel A). The representative dark-field photomicrographs show the expression of *Vmat2* mRNA in the substantia nigra (SN) and ventral tegmental (VTA), the dorsal raphe nucleus (RAPHE), and in the locus coruleus (LC) in a wild-type mouse. No signal was detected in the homozygous KA1 mutant.

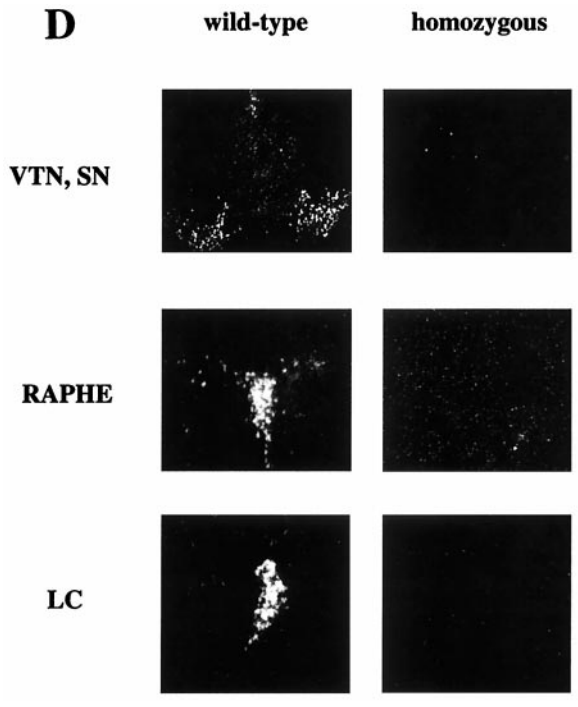

FIG. 1—*Continued.*

arm of the construct did not recombine as predicted but inserted into the *Vmat2* locus (Fig. 1A). The insertion site was confirmed by Southern blot analysis by using 3′ and 5′ hybridization probes (Fig. 1B) and verified by PCR analysis of the junction between the transgene and the genome (Fig. 1C).

Generation of chimeric KA1 and GB1/1 mice. Chimeric mice were generated by injection of the selected ES cells into blastocysts of C57BL/6 mice using standard techniques (29). Highly chimeric males were bred with C57BL/6 females, and agouti offspring were tested for germ line transmission by Southern blot analysis of DNA extracted from tail-tip specimens. Homozygous mice were obtained by interbreeding heterozygotes. In all subsequent experiments, the genotype of the mice was confirmed by Southern blot analysis of tail tips.

In situ hybridization histochemistry. Brains from adult mice were removed, rapidly frozen, and stored at −70°C. Ten-micrometer sections were cut (cryostat) and processed for in situ hybridization by using a mix of four different ^{35}S-labeled oligonucleotide probes directed against mouse *Vmat2* mRNA: 5′-GCAGCAGC ACCAGATCGCTCAGGGCCAT-3′ (exon 1, nucleotides 1 to 24); 5′-GGATC AGCTTGCGCGAGTGGCGGCTGTCCCGCAGCC-3′ (exon 1, nucleotides 28 to 63); 5′-GCCTTGGGTGACTCCCCTCCTGGGAGGCCCCCCCGT GGC-3′ (exon 2, nucleotides 272 to 310); and 5′-CATTTATGCAGAATCCAGCAAAC ATGG GAATTGGATAGCC-3′ (exon 2, nucleotides 179 to 218) (33). Enkephalin mRNA was detected with ^{35}S-labeled antisense oligonucleotide probes for mouse proenkephalin cDNA (nucleotides 2428 to 2463; GenBank accession number U09941), and substance P mRNA was detected with ^{35}S-labeled oligonucleotide probes antisense to mouse beta-preprotachykinin A cDNA (nucleotides 234 to 270; GenBank accession number D1007723). Hybridization was carried out in 2× SSC (1× SSC is 0.15 M NaCl plus 0.015 M Sodium citrate), 50% deionized formamide, 10% dextran sulphate, 250 μg sonicated salmon testes DNA/ml, 1× Denhardt's solution, and 3% β-mercaptoethanol with a probe concentration of 100,000 dpm/μl at 37°C in a humidified chamber. The sections were washed three times with 1× SSC at 55°C for 30 min and with 1× SSC at room temperature (RT) for 1 h. Dehydrated sections were exposed to Kodak β-Max autoradiography film at RT for 4 to 21 days. After development of the film, the sections were coated with nuclear track emulsion (Ilford K2) in the dark and stored at 4°C in the dark. Quantification of the hybridization signal was carried out by counting silver grains on individual cells with the SeeScan microautoradiography system (Cambridge, United Kingdom).

Immunohistochemical analysis. Brains from adult mice were removed, fixed in 4% paraformaldehyde (PFA) for at least 12 h at 4°C, and then kept in 30% sucrose in phosphate-buffered saline (PBS). Fifty-micrometer sections were cut and processed for immunohistochemistry using a 1:1000 dilution of an affinity-purified rabbit polyclonal antiserum with antibodies raised against a synthetic peptide from the intracellular C-terminal region of the human *VMAT2* gene (Chemicon). VMAT2 immunoreactivity visualized by this *VMAT2* antiserum was detected in all the major monoaminergic cell groups in the brain, as expected (28). Tyrosine hydroxylase (TH) immunoreactivity was visualized using a monoclonal anti-TH antibody purchased from Sigma (mouse ascites fluid clone TH-2). Preliminary quantification of TH-immunopositive cells in the substantia nigra and ventral tegmental areas were made using unbiased dissector methods with an Olympus optical dissector-stereology package.

RT-PCR analysis. Total midbrain RNA from homozygous and wild-type GB1/1 and KA1 neonates was isolated using a Qiagen RNA purification kit and reverse transcribed with Superscript II reverse transcriptase (RT) and random primer oligonucleotides (mostly hexamers) (Gibco BRL) under recommended conditions. Of the first strand reaction mixture, 10% was used for PCR with *Taq* DNA polymerase (Qiagen). The primers used for the PCR amplification of the first strand reaction were designed according to the mouse *Vmat2* cDNA sequence in the second exon (5′-GCTACCTGTACAGCATTAAGCACG-3′) for the forward primer and in exon 12 for the reverse primer (5′-CCAACTCCAA AGTTGGGAGCG-3′) (33), and according to the mouse *Hprt* cDNA sequence at nucleotide position 346 (5′-CCTGCTGGATTACATTAAAGCACTG-3′) for the forward primer and at nucleotide position 714 (5′-GTCAAGGGCATATC CAACAACAAAC-3′) for the reverse primer (22). RT-PCR amplification conditions were denaturing for 2 min at 94°C followed by 36 cycles of 1 min at 94°C, 1 min at 60°C, and 1 min at 72°C.

Western blot analysis. Membrane proteins were prepared from the striatum of wild-type and KA1 homozygous mutant mice. The tissue was homogenized using a Waring blender in 10 volumes of homogenizing buffer (50 mM HEPES, 1 mM disodium EDTA, 1 mM EGTA) containing 1 mM phenylmethylsulfonyl fluoride and 1 mM pepstatin and centrifuged at 1,000 × *g* and the pellet was discarded. The membrane fraction was retrieved by centrifugation at 40,000 × *g*, washed twice in the homogenization buffer, and finally resuspended in the same buffer to a concentration of 20 mg/ml and stored at −80°C. The protein content was determined using the Bio-Rad Bradford reagent protocol. A total of 30 μg of protein of each membrane vesicle preparation was separated by electrophoresis through polyacrylamide and transferred to nitrocellulose by electroblotting. The blot was incubated with a crude rabbit antiserum with antibodies raised against a peptide present in the human *VMAT2* gene at a 1:1000 dilution. As a control for the amount of loaded protein, an identical gel was run in parallel and stained with Coomassie blue (data not shown).

Quantification of brain monoamines. Dissected brain regions were sonicated in 0.1 M perchloric acid and 0.1 mM EDTA (10 mg/100 μl). The extracts were then centrifuged for 15 min and the supernatant was collected and stored at −20°C. Monoamines (noradrenaline, dopamine, serotonin) and metabolites (dihydroxyphenylacetic acid [DOPAC], homovanillic acid [HVA], and 5-hydroxyindolacetic acid [5-HIAA]) were measured with high-pressure liquid chromatography (HPLC) using electrochemical detection as described previously (12).

Behavioral testing. All mice were weaned at 21 days of age and housed with two to five same-sex littermates. Male mice were used in the behavioral testing. All animals were maintained on a 12-h light-dark cycle (lights on at 0700 to 1900) and were permitted free access to food and water. Beam walking was assessed using 1-m-long wooden beams suspended 80 cm from the floor. The mice were placed on one end of the beam, and the time taken to reach the other end (where the mice entered a cardboard shelter) was assessed. The number of slips and falls in negotiating the beams were also recorded. Task difficulty was increased by altering the diameter and shape of the beams (from least to most difficult): 15-mm round, 10-mm square, and 10-mm round beams. In order to ensure the animals were fully habituated to the test situation, training took place over 4 days, with the more difficult beams being gradually introduced. On day 4 (test day), the mice were given six attempts on each of the beams. The data presented are the mean of the six attempts. Novelty place preference was assessed in an apparatus with two 29 by 29 by 29-cm compartments, each separated by a small central compartment. Each main compartment was distinguished by color (black or white) and flooring (sandpaper or smooth). During the test, the mouse was placed in one or the other compartment for 60 min, making it familiar relative to the other unexplored and therefore novel side. Then the mice were given a free choice between both compartments for 10 min, and the time spent in the novel side, the number of visits made, and the number of exploratory rears when in the novel side were measured. Stereotyped behaviors following the intraperitoneal (i.p.) injection of *d*-amphetamine sulphate (3 mg of free base/kg of body weight) were assessed blind from videotapes by using a scoring system based on that used by Mittleman et al. (23). Behavior was monitored for 1 h postinjection in specially adapted Perspex boxes.

MPTP treatment. For this experiment, only male mice backcrossed into C57BL/6 for five generations were used. Three doses of 1-methyl-4-phenyl-1,2,3,6-tetrahydropyridine (MPTP) (Sigma M-0896) were administered i.p. 16 mg/kg, 3 h apart. Two control mice in each group received three i.p. injections of saline. Mice were kept on heated blankets for 24 h after the injections and culled 8 days after drug treatment. All mice were perfused with PBS and 4% PFA. The brains were removed, fixed in 4% PFA for 12 h at 4°C, and then stored in 30% sucrose in PBS. Fifty-micrometer sections were cut and processed for immunohistochemistry using a 1:1000 dilution of a TH antibody (Sigma T-1299). Sections were dried and mounted in Depex. Cell counting was performed using a computer-assisted stereological toolbox (CAST-Grid; Olympus). All cell counts were done blind to genotypes and drug treatments and performed at 100-fold magnification.

RESULTS

Generation of KA1 and GB1/1 transgenic mice. To generate VMAT2-deficient mice, we used a replacement vector containing sequences homologous to the *Vmat2* target sequences with a neomycin resistance (*neo*) expression cassette inserted within the region of homology (Fig. 1A). The expected double-reciprocal recombination resulted in deletion of exons 1 and 2 and flanking intron sequences and a replacement of the deleted region with the *neo* cassette (see Fig. 3B). Homozygous mice derived from these clones (GB1/1 mice) died, as has been previously reported with *Vmat2* knockouts soon after birth (9, 34, 36). However, we also identified a clone (KA1) that carried a hypomorphic *Vmat2* allele, in which a single recombination occurred on one arm of the construct and resulted, as detailed in Fig. 1A, in an insertion of the *neo* cassette and of the leader exon with 5′ flanking sequences of the construct into the third intron of the *Vmat2* gene. Probes for 5′ and 3′ flanking sequences of the insertion detected polymorphic restriction fragments of the expected sizes in transgenic tail DNA with all enzymes tested (Fig. 1B). Insertion of exogenous DNA is known to result in deletions of neighboring sequences of the endogenous DNA. To examine this possibility in the KA1 mice, primers were designed to use PCR to analyze the junction between the transgene and 5′ flanking sequence. The sequence of the PCR product is given in Fig. 1C. The sequence comparison of the PCR product with the cloned genomic region revealed the location of the insertion as well as a deletion of 245 bp from the 5′ end of the transgene. The other arm of the targeting construct and sequences 3′ from the insertion event stayed intact after homologous recombination. Using the 3′ probe, no differences in the hybridization patterns between the knockout line GB1/1 and KA1 could be found with any enzymes tested (data not shown), indicating that the single recombination event did not cause any major deletions and/or rearrangements in the endogenous *Vmat2* gene. Mice derived from clone KA1 were able to survive with the mutation on both alleles (homozygotes) and were used in the present studies at between 3 and 6 months of age.

VMAT2 expression in KA1 mice. The insertion of the transgene construct in the KA1 mice was effective in blocking *Vmat2* expression, as confirmed by Northern blotting (data not shown), in situ hybridization, and immunohistochemical evidence from brain sections (Fig. 1D and 2). In situ hybridization of brain sections with oligonucleotides complementary to the *Vmat2* message indicated an absence of *Vmat2* mRNA in the major monoaminergic cell body groups in the brain of homozygous KA1 mice (Fig. 1D); this was confirmed by immunocytochemistry by using a VMAT2 antibody to show that no VMAT2 protein was detectable in the midbrain and striatal regions of the brain in the mutant mice, although it was readily detectable in wild-type littermates (Fig. 2). However, the presence of the monoamine cells in the substantia nigra and their processes in the striatum in homozygous KA1 mice could be readily visualized with an anti-TH antibody. Furthermore, no reduction in the number of TH-positive cells could be detected using an unbiased counting method, performed by using the computer-assisted stereological toolbox (CAST-Grid) system from Olympus. TH-immunopositive cells were counted from 30 serial sections (50 μm) in the A8, A9, and A10 regions from five animals homozygous for the KA1 insertion and four wild-type mice. Total cell counts (mean ± standard error of the mean [SEM]) were 15,980 ± 1,305 for the wild-type ($n = 4$) and 16,328 ± 1,102 for the homozygous animals ($n = 5$). There was no significant difference in the number of cells between the two groups (Student's t test). PCR amplification of cDNA made from homozygous KA1 and GB1/1 brain RNA with *Vmat2*-specific primers detected normal transcripts in homozygous KA1 neonates but not in homozygous GB1/1 neonates (Fig. 3A). Sequence analysis of the KA1 PCR amplification product confirmed that an intact correctly spliced message can be generated from the KA1 allele. This result indicates that VMAT2 may be expressed, but at very low levels. Although no residual VMAT2 protein could be detected using a polyclonal *VMAT2* antibody in immunohistochemical analyses, residual amounts of VMAT2 protein could be detected with Western blots of purified vesicle membrane proteins from the striatum of homozygous KA1 mice (Fig. 3C). Enhanced chemiluminescence Western blotting analysis detected background bands of higher molecular weight in both samples, whereas the smaller (≈55 kDa) VMAT2-specific band, which was readily detectable in the wild-type mouse, was barely detectable in the homozygous KA1 mutant.

Monoamine brain chemistry in VMAT2-deficient KA1 mice. The loss of VMAT2 expression in the viable KA1 mice was associated with large reductions in the brain concentrations of the monoamine transmitters. Figure 4 illustrates the pattern of neurochemical changes seen in selected brain areas. There were general reductions in tissue levels of dopamine, noradrenaline, and serotonin, which in most brain regions were dependent on gene dosage. Whilst there were also reductions in the main metabolites, HVA, DOPAC, and 5-HIAA, it was noticeable that the ratio of metabolites to transmitter was in many cases increased, suggesting an increased turnover of monoamines in homozygous mice. Quantitative analysis of TH immunohistochemistry (Fig. 2) indicated that, at the age tested (3 to 6 months), the reduced levels of dopamine in terminal and cell body regions of the VMAT2-deficient mice occurred in the absence of any significant loss of dopamine cell bodies in the substantia nigra and ventral tegmental area, suggesting that it was, in the main, the abnormal handling of dopamine by the vesicles that was responsible for the reductions in transmitter content.

Motor functioning in VMAT2-deficient KA1 mice. Basic visual inspection of the VMAT2-deficient mice indicated no obvious physical abnormalities compared to wild-type controls, though they did weigh less at the time of testing (wild type, 35.1 ± 1.32 g; heterozygous, 33.15 ± 1.72 g; homozygous, 29.24 ± 1.14 g). However, motor deficits became apparent in a

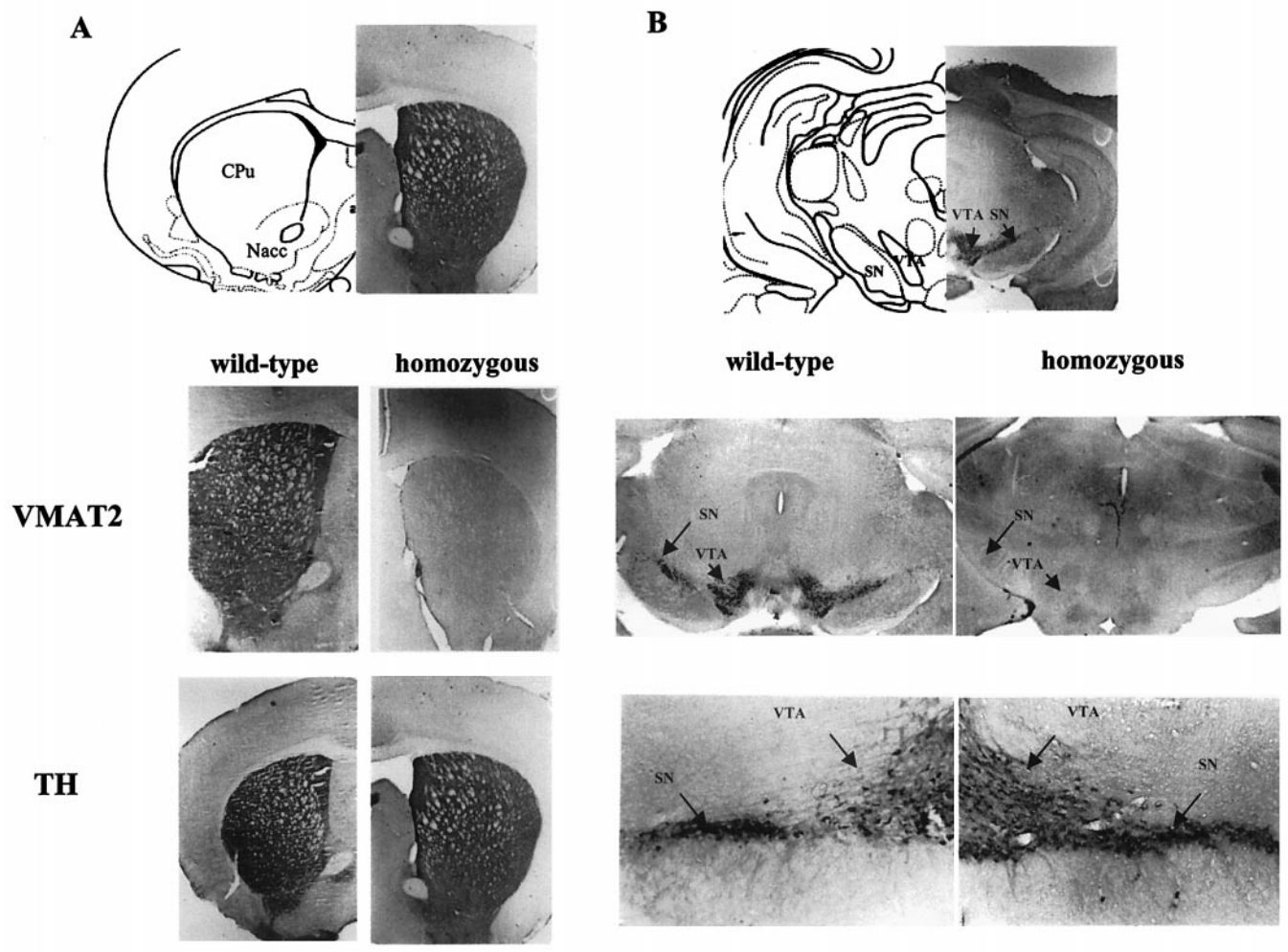

FIG. 2. VMAT2 and TH immunoreactivity in striatal and midbrain regions of KA1 homozygous mice. (A) Striatal sections from wild-type and homozygous KA1 mice were stained for VMAT2 immunoreactivity (VMAT2) using a specific antiserum. VMAT2 immunoreactivity is present in the caudate putamen (CPu) and the nucleus accumbens (Nacc) of wild-type mice but absent in those structures in homozygous mice. In striatal sections from wild-type and homozygous KA1 mice stained for TH immunoreactivity using a specific antiserum, the level of TH immunoreactivity in the caudate putamen and the nucleus accumbens was similar in both wild-type and homozygous mice. (B) VMAT2 immunostaining is absent in the substantia nigra (SN) and the ventral tegmental area (VTA) of the homozygous KA1 mouse and present in the wild-type mouse, whereas TH immunoreactivity is also present in the dopamine cell body region of homozygous mice. The apparent lack of differences in TH immunoreactivity between wild-type and homozygous mice, seen on gross visual inspection, was confirmed by quantitative analysis of four wild-type and five homozygous animals.

beam walking task, a sensitive test of motor coordination and balance, whereby VMAT2-deficient KA1 mice took longer and made more slips in crossing narrow wooden beams suspended 80 cm from the floor (Fig. 5A). The effects on motor performance were probably largely independent of motivational factors, since the beam walking training protocol allowed for substantial habituation to the test situation with gradually increasing levels of difficulty. Moreover, the VMAT2-deficient KA1 mice showed normal reactivity in a novelty place preference task, as indexed by the time spent in the novel as opposed to the familiar environment (Fig. 5A). This was despite evidence of a general reduction in locomotor activity in the task, as indexed by crossings and rears within the test apparatus (Fig. 5A). Novelty place preference was assessed in an apparatus with two 29 by 29 by 29-cm compartments distinguished by color (black and white) and sandpaper flooring on one side. After 60 min of habituation in one of the compartments, an opening was made available for access to the other compartment. Time spent in the novel chamber as well as the number of visits into the novel environment and the number of rears in the novel place were recorded for 10 min. There were no significant group differences in the time spent on the novel side of the test apparatus. There were, however, significant group differences between homozygous, heterozygous, and wild-type mice in the number of visits and rears in the novel environment. The ability of the VMAT2-deficient mice to make the distinction between a novel and a familiar environment also argued against confounds in the interpretation of motor effects arising from underlying sensory deficits.

Enhanced amphetamine-induced stereotypy in VMAT2-deficient KA1 mice concurrent with altered chemical neuroanatomy in the striatum. The VMAT2-deficient KA1 mice also

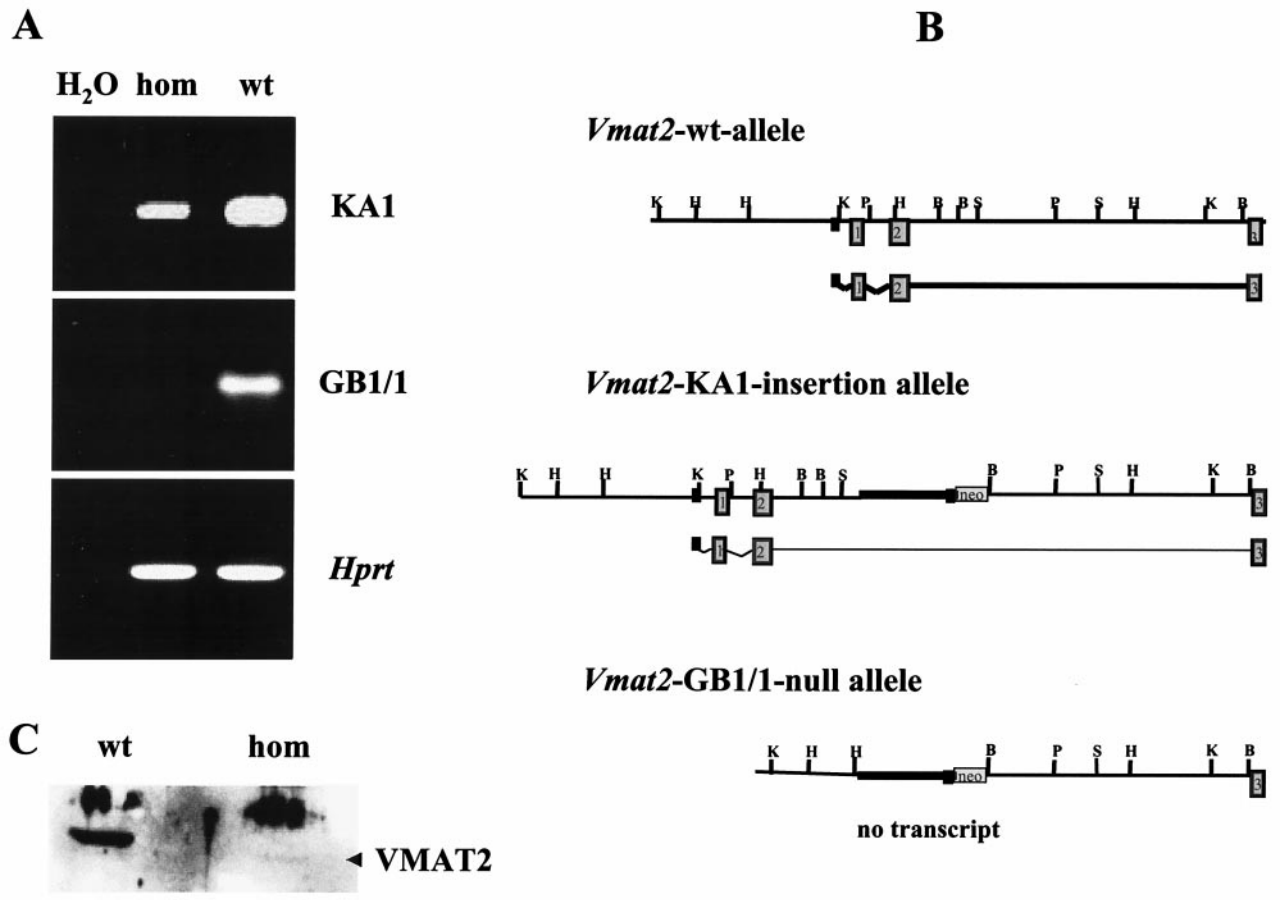

FIG. 3. RT-PCR and Western blot analysis of homozygous KA1 insertional mutants and homozygous GB1/1 knockout mice. (A) Ethidium-stained agarose electrophoresis of RT-PCR products. Total midbrain RNA from homozygous (hom) and wild-type (wt) GB1/1 and KA1 neonates was isolated and reverse transcribed. Expression of *Vmat2* mRNA was detected using specific primers for exon 2 and exon 12 of the mouse *Vmat2* gene (33). These primers amplified *Vmat2* cDNA made from homozygous KA1 mice, but no amplification product was generated with cDNA made from homozygous GB1/1 neonates. The quality of all cDNA preparations was examined by performing control RT-PCRs with primers to hypoxanthine phosphoribosyltransferase (*Hprt*) (22). (B) Schematic representation of the genomic organization of the *Vmat2* wild-type allele, the KA1 insertion allele, and the GB1/1 knockout allele. The wild-type allele is transcriptionally active. The KA1 insertion interferes severely with transcription, and only a small amount of *Vmat2* message is generated. In the GB1/1 knockout line, the first and second exon of the *Vmat2* gene are deleted, completely abolishing the generation of normal *Vmat2* message. (C) Western blot of striatal membrane preparations from homozygous and wild-type KA1 mice probed with a polyclonal antibody against the VMAT2 protein. Both lanes contain comparable amounts of protein, as determined by the Bradford method. Quantitative analysis of the blot using SeeScan indicated a decrease in signal of more than 95% in homozygotes below that of the wild-type signal. The position of the VMAT2-specific band is indicated by the arrowhead. The higher molecular weight band is nonspecific, being found in extracts from controls and mutants.

showed enhanced stereotypic behaviors in response to the dopamine releasing drug *d*-amphetamine (Fig. 5B). Homozygous KA1 mice showed a dramatically increased responsiveness to a single *d*-amphetamine injection (3 mg/kg) given i.p., resulting in increased stereotyped behaviors of these mice compared to their wild-type and heterozygous littermates. No group differences were detected in response to saline injections, indicating that these effects were unlikely to be due to preexisting differential reactivities to the i.p. injections per se (data not shown). Dopamine effects in dorsal striatum are a key substrate for behavioral stereotypies (30), so we examined molecular neuroanatomical indices of dopamine function in this structure for possible correlates of the altered sensitivity to amphetamine. Whilst there were no differences in gene expression of dopamine receptors of the D1 and D2 subtypes (data not shown), there was evidence, as illustrated in Fig. 5C, of changes in mRNA levels of substance P and enkephalin, peptides which distinguish between the two main output pathways from the striatum, the striatonigral (direct) and striatopallidal (indirect) pathways (11). As illustrated with in situ hybridization in Fig. 5C, homozygous VMAT2-deficient mice showed a striking down-regulation of substance P mRNA and an up-regulation of enkephalin mRNA in the striatum, giving rise, in turn, to the possibility of abnormalities in the organization of dopamine-mediated signaling via direct and indirect efferents.

Increased toxin sensitivity in midbrain of KA1 homozygous mice. We noted that in several ways the VMAT2-deficient KA1 mice modeled aspects of the symptomatology of Parkinson's disease, namely in terms of a lowered brain content of monoamines, especially dopamine (14), the presence of motor deficits (27), and the pattern of changes in peptides associated with the direct (substance P) and indirect (enkephalin) output

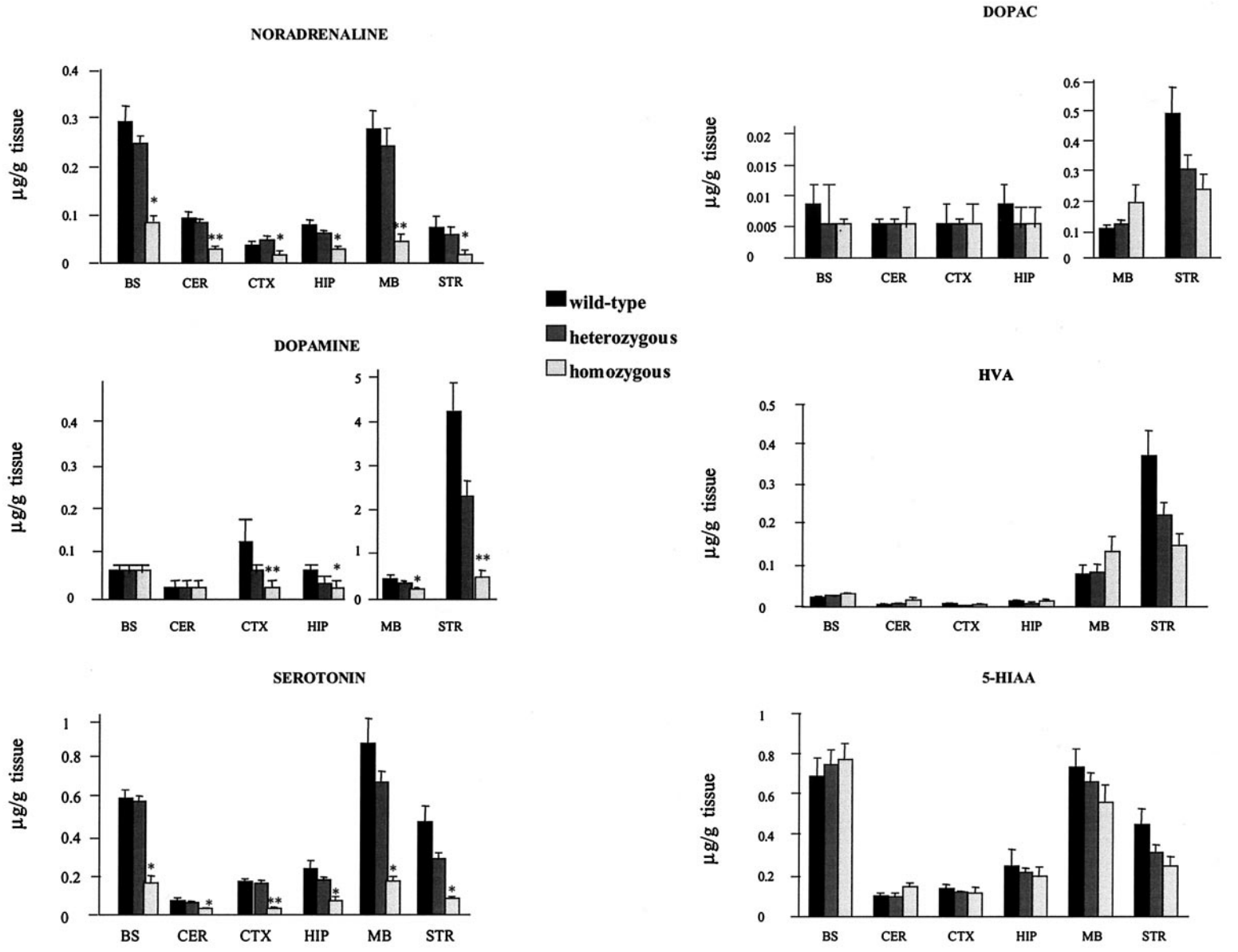

FIG. 4. Quantification of monoamines and metabolites in different brain regions of wild-type, heterozygous, and homozygous mice. Dopamine, noradrenaline, and serotonin, as well as their main metabolites, DOPAC, HVA, and 5-HIAA, were measured in perchloric acid extracts prepared from brain areas of 13 wild-type, 17 heterozygous, and 6 homozygous mice using HPLC with electrochemical detection (12). In comparison to wild-type controls, KA1 homozygous mice showed widespread, major reductions in the levels of all three monoamines. The results are represented as the mean ± SEM. *, $P < 0.05$; **, $P < 0.001$, compared with the wild-type group (Student t test). In contrast, metabolite levels of all three monoamines were, in general, much less affected in the VMAT2-deficient KA1 mice, consistent with higher rates of monoamine turnover in these animals.

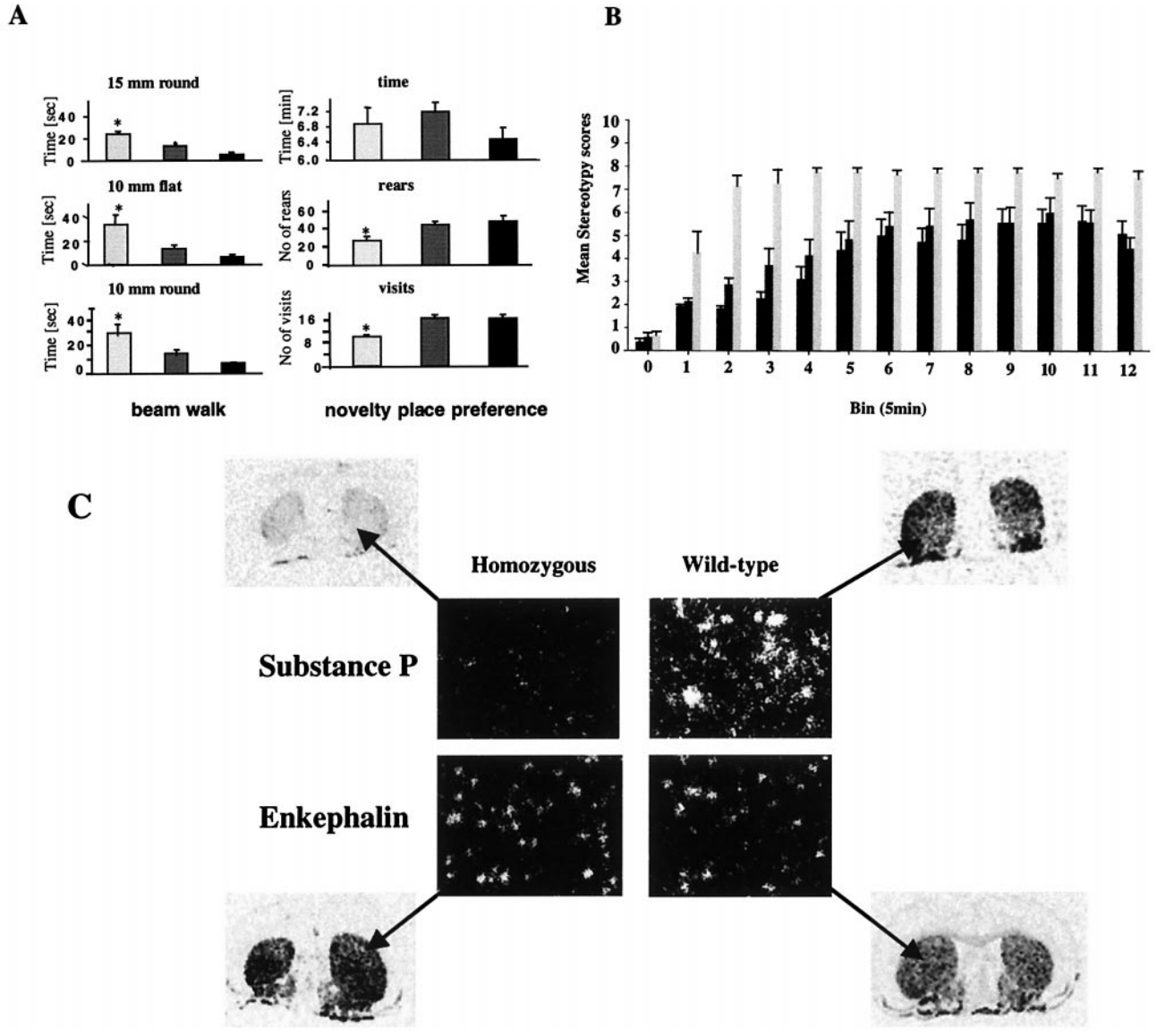

FIG. 5. Motor functioning and dopamine supersensitivity in KA1 mice. (A) Homozygous (light gray bars) and heterozygous (dark gray bars) KA1 mice could not perform as well as their wild-type (black bars) littermates in a beam walking task, but they showed a normal preference for a novel environment. The results, for each beam diameter and shape, are the mean latencies to cross the beam ± SEM of six crossings done by 15 males of each genotype in the fourth (i.e., the final) test session. Data were analyzed by the Tukey-Kramer multiple comparison test, which indicated significant group differences at each level of difficulty (*, $P < 0.05$; **, $P < 0.001$, compared with the wild-type group [Student t test]). The novelty place preference, assessed using the Tukey-Kramer multiple comparisons test, did not show any significant group differences in the time spent on the novel site. There were, however, significant group differences in the number of visits and rears in the novel environment. The results are represented as mean ± SEM for 15 mice of each genotype. *, $P < 0.05$; **, $P < 0.001$, compared with the wild-type group (Student t test). (B) Increased responsiveness to systemically administered d-amphetamine (3 mg/kg) given i.p., on stereotyped behaviors in wild-type, heterozygous, and homozygous animals. Stereotypy ratings, based on the scoring system of Mittleman et al. (23), were taken blind for 1 h postinjection. The lower the rating, the lower the observed rate of stereotypy, and vice versa. The results are the mean scores ± SEM, registered in 12 5-min bins, for 11 wild-type, 8 heterozygous, and 9 homozygous mice. Analysis of variance indicated a significant main effect of group ($P < 0.01$), consistent with an increased response to d-amphetamine in the homozygous mice. (C) An altered chemical neuroanatomy in the striatum of male VMAT2-deficient KA1 mice expressing substance P and enkephalin mRNA is shown in striatal sections from wild-type mice and homozygous KA1 mutants, hybridized with oligonucleotides complementary to the substance P and enkephalin messages. The relative down-regulation of substance P mRNA expression and the relative up-regulation of enkephalin mRNA expression in the striatum of KA1 homozygous mice was quantified by silver grain counting on mRNA-positive cells. The difference between the two groups was compared by the Student t test and showed a significant difference in the number of silver grains per square millimeter of cell area between wild-type and homozygous mice for both substance P ($P < 0.001$) and enkephalin ($P < 0.05$).

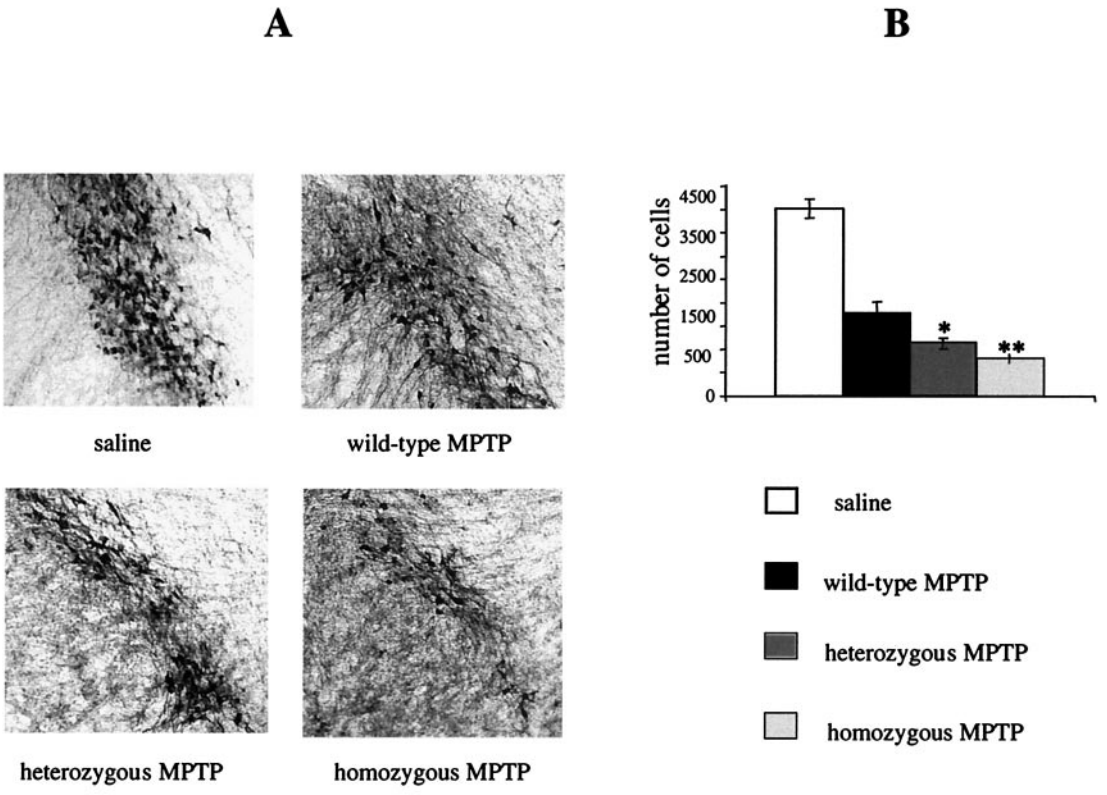

FIG. 6. MPTP treatment of wild-type, heterozygous, and homozygous KA1 mice. (A) TH-immunopositive cells in sections from the substantia nigra pars compacta of saline-treated and MPTP-treated wild-type, heterozygous, and homozygous KA1 mice. (B) Number of TH-immunopositive cells in the substantia nigra pars compacta of saline-treated and MPTP-treated wild-type, heterozygous, and homozygous KA1 mice. TH-immunopositive cells were counted from 30 serial sections from 4 wild-type, 3 heterozygous, and 3 homozygous MPTP-treated and 4 saline-treated (2 homozygous and 2 wild-type) mice. The cell loss was significantly increased in MPTP-treated heterozygous and homozygous KA1 mice compared to the MPTP-treated wild-type littermates. The difference between the three groups was compared by the Student *t* test and showed a significant difference in the number of TH-positive cells between wild-type and heterozygous MPTP-treated mice ($P < 0.01$) and between wild-type and homozygous MPTP-treated mice ($P = 0.001$).

pathways of the striatum (8, 17). However, the mice did not exhibit overt dopamine cell loss in midbrain areas (Fig. 2), the classical finding in Parkinson's disease (4). We were interested to see, therefore, whether the mice have a lowered threshold for dopamine cell damage caused by using the neurotoxin MPTP (15). As shown in Fig. 6, this was found to be the case, as significantly more dopamine cell loss occurred in the substantia nigra and the ventral tegmental area of the VMAT2-deficient mice following toxin administration compared to responses in their heterozygous and wild-type littermates. We are currently examining the possibility that a similar underlying vulnerability to damaging events may be manifest with increasing age of the mice. Such findings would be consistent with the usual history of idiopathic Parkinson's disease, in which age is a major risk factor (31), and may also bear on recent speculation about VMAT2 and its role in mediating efficient clearance of dopamine in the selective vulnerability of midbrain dopamine neurons in the disease (18, 35).

DISCUSSION

We describe here the development of a mouse line which, according to analyses by in situ hybridization and immunohistochemical methods, does not express detectable levels of VMAT2 and which, in contrast to other reported knockouts of the *Vmat2* gene (9, 34, 36), survives as homozygotes into adulthood without gross physical deficits. The reason why the mice survive is related to the nature of the recombination event and the observation that the suppression of gene expression is not complete. KA1 homozygous mice survive because the insertion event in this line differs from that in the GB1/1 line in permitting residual expression of *Vmat2*, which was low enough to escape detection by Northern blotting, in situ hybridization, and immunohistochemical methods but which was sufficient to rescue the mouse. Consistent with this explanation, a more sensitive RT-PCR method did reveal low levels of endogenous *Vmat2* message in the KA1 line that was absent in the GB1/1 line (Fig. 3A). Also, extremely low levels of protein could be detected in Western blots in striatal membrane proteins isolated from homozygous KA1 mice (Fig. 3C). A precedent for this rescue has recently been reported where an insertion into intron 20 of the N-methyl-D-aspartate receptor subunit NR1 resulted in mice with only 5% of normal expression levels. These mice have been used to study schizophrenia-like behavioral abnormalities (24), whereas the NR1 knockout mice die perinatally (10). That this small amount of protein may be functionally active in the KA1 mice was confirmed by fast cyclic

voltammetry on coronal striatal slices prepared from homozygous KA1 mutants and wild-type littermates, where small amounts of vesicular dopamine released in homozygotes could be measured (J. A. Stamford and J. Patel, personal communication). Whilst the residual expression of VMAT2 in the KA1 line rescued the lethal phenotype, the mice were not normal.

The survival of the VMAT2-deficient KA1 mice allowed us to examine the effects of abnormalities in the main intracellular uptake mechanism for handling monoamine neurotransmitters in the adult, homozygous animal. A major brain phenotype was a profound reduction in the levels of monoamine transmitters. In the case of dopamine, we ascertained that these neurochemical changes occurred in the absence of any overt loss of dopamine cell bodies, suggesting that it was, in the main, the abnormal handling of dopamine by the vesicles that was responsible for the reductions in transmitter content. The changes in brain monoamine metabolism were accompanied by motor deficits and an enhanced behavioral responsiveness to *d*-amphetamine, manifest as increased stereotypy. The increased sensitivity to *d*-amphetamine did not appear to be related to changes in striatal dopamine receptors of the D1 or D2 type (data not shown). However, we did observe large effects on substance P and enkephalin gene expression in VMAT2-deficient KA1 mice, which may be indicative of an altered functional architecture in the striatum. In our mouse model, small amounts of vesicular and nonvesicular dopamine released in response to *d*-amphetamine might act on "supersensitive" dopamine receptors of the direct and/or indirect striatal efferents, giving rise to an overall enhanced effect of dopamine agonism, which is expressed as behavioral stereotypy. The enhanced sensitivity of the KA1 mice to *d*-amphetamine may also have been related to changes in presynaptic function, such as increased dopamine transport into or out of the cell, which can be measured but which we did not attempt to measure in the present work. The KA1 mouse models in several ways aspects of the symptomatology of Parkinson's disease, namely, in terms of a lowered brain content of monoamines, especially dopamine (14), the presence of motor deficits (27), and the pattern of changes in peptides associated with the direct (substance P) and indirect (enkephalin) output pathways of the striatum (8). Together with electrophysiological data (1), effects on the chemical neuroanatomy of the striatum form a major part of the evidence indicating a key role for perturbations in the balance of the direct and indirect pathway functioning in the motor abnormalities present in Parkinson's disease (17), a theoretical standpoint which provides the basis for the recent surgical approaches to treating the condition (2) and may also provide some insight into the ameliorative properties of L-DOPA (13). It is, therefore, particularly noteworthy that the VMAT2-deficient KA1 mice showed qualitatively similar changes in striatal substance P and enkephalin expression to the human disease, as well as to other animal models of Parkinson's disease that also result in reduced brain dopamine, such as the administration of the toxins MPTP and 6-hydroxydopamine to monkeys (15) and rats (37), respectively.

It is also clear that in several other ways the KA1 mice do not model the typical features of Parkinson's disease. There was no evidence of dopamine cell loss in the substantia nigra, and the mice, whilst being mildly akinetic, showed no signs of resting tremor or rigidity. This may be due to the relatively young age of the mice when tested (3 to 6 months), and we are currently examining the possibility that larger motor deficits, perhaps with concurrent loss of dopamine cells, will develop as the animals age. Such findings would be consistent with the usual history of idiopathic Parkinson's disease, where age is a major risk factor (31), and may also bear on recent speculation about VMAT2 and its role in mediating efficient clearance of dopamine in the selective vulnerability of nigral neurons in the disease (35). Our VMAT2-deficient KA1 mice do indeed model such a form of neuronal vulnerability, which manifests itself as the emergence of frank pathology not only in old animals but also in young animals subjected to additional toxic insults such as MPTP. The titration of vulnerability thresholds and the direct contribution made by VMAT2 functioning to variation in the thresholds epitomize the potential value of our mice in being able to examine, long term, the insidious damaging consequences of abnormal intracellular handling of monoamines. On the basis of our present findings, these mice are likely to prove of immediate interest to models of Parkinson's disease. They may also, however, be of use in probing other aspects of monoaminergic function and dysfunction in brain, the latter making important contributions to the study of the pathogenesis of schizophrenia and addiction.

ACKNOWLEDGMENTS

We thank Carlos de la Riva and Michael Hinton for their excellent technical assistance in generating and interpreting the HPLC data.

This work was funded by the Biotechnology and Biological Sciences Research Council, United Kingdom, and the Parkinson's Disease Society, United Kingdom (grant 3094 to P. C. Emson and L. S. Wilkinson). N. D. Allen is a BBSRC Advanced Fellow. All animals in this study were treated in accordance with the United Kingdom Animal (Scientific Procedures) Act of 1986.

REFERENCES

1. **Bergman, H., A. Feingold, A. Nini, A. Raz, H. Slovin, M. Abeles, and E. Vaadia.** 1998. Physiological aspects of information processing in the basal ganglia of normal and parkinsonian primates. Trends Neurosci. **21:**32–38.
2. **Bergman, H., T. Wichmann, and M. R. DeLong.** 1990. Reversal of experimental parkinsonism by lesions of the subthalamic nucleus. Science **249:** 1436–1438.
3. **Björklund, A., and O. Lindvall.** 1975. Dopamine in dendrites of substantia nigra neurons: suggestions for a role in dendritic terminals. Brain Res. **83:**531–537.
4. **Chase, T. N., J. D. Oh, and P. J. Blanchet.** 1998. Neostriatal mechanisms in Parkinson's disease. Neurology **51:**30–35.
5. **Dahlström, A., and K. Fuxe.** 1964. Evidence for the existence of monoamine-containing neurons in the central nervous system. 1. Demonstration of monoamines in the cell bodies of brain stem neurons. Acta Physiol. Scand. Suppl. **62:**232.
6. **Egan, M. F., and D. R. Weinberger.** 1997. Neurobiology of schizophrenia. Curr. Opin. Neurobiol. **7:**701–707.
7. **Erickson, J. D., L. E. Eiden, and B. J. Hoffman.** 1992. Expression cloning of a reserpine-sensitive vesicular monoamine transporter. Proc. Natl. Acad. Sci. USA **89:**10993–10997.
8. **Fernandez, A., M. L. de Ceballos, S. Rose, P. Jenner, and C. D. Marsden.** 1996. Alterations in peptide levels in Parkinson's disease and incidental Lewy body disease. Brain **119:**823–830.
9. **Fon, E. A., E. N. Pothos, B.-C. Sun, N. Killeen, D. Sulzer, and R. H. Edwards.** 1997. Vesicular transport regulates monoamine storage and release but is not essential for amphetamine action. Neuron **19:**1271–1283.
10. **Forrest, D., M. Yuzaki, H. D. Soares, L. Ng, D. C. Luk, M. Sheng, C. L. Stewart, J. I. Morgan, J. A. Connor, and T. Curran.** 1994. Targeted disruption of NMDA receptor 1 gene abolishes NMDA response and results in neonatal death. Neuron **13:**325–338.
11. **Gerfen, C. H.** 1992. The neostriatal mosaic: multiple levels of compartmental organization in the basal ganglia. Annu. Rev. Neurosci. **15:**285–320.
12. **Guevara-Guzman, R., P. C. Emson, and K. M. Kendrick.** 1994. Modulation of in vivo striatal transmitter release by nitric oxide and cyclic GMP. J. Neurochem. **62:**807–810.

13. **Herrero, M. T., S. J. Augood, E. C. Hirsch, F. Javoy-Agid, M. R. Luquin, Y. Agid, J. A. Obeso, and P. C. Emson.** 1995. Effects of L-DOPA on preproenkephalin and preprotachykinin gene expression in the MPTP-treated monkey striatum. Neuroscience **68:**1189–1198.
14. **Hornykiewicz, O.** 1966. Metabolism of brain dopamine in human parkinsonism: neurochemical and clinical aspects, p. 171–185. *In* X. Costa, L. J. Côté, and M. D. Yahr (ed.), Biochemistry and Pharmacology of the basal ganglia. Raven Press, New York, N.Y.
15. **Jolkkonen, J. P., Jenner, and C. D. Marsden.** 1995. L-DOPA reverses altered gene expression of substance P but not enkephalin in the caudate-putamen of common marmosets treated with MPTP. Mol. Brain Res. **32:** 297–307.
16. **Koob, G. F., and M. Le Moal.** 1997. Drug abuse and alcoholism. Overview. Science **278:**52–58.
17. **Levy, R., L. N. Hazrati, M. T. Herrero, M. Vila, O. K. Hassani, M. Mouroux, M. Ruberg, H. Asensi, Y. Agid, J. Feger, J. A. Obeso, A. Parent, and E. C. Hirsch.** 1997. Re-evaluation of the functional anatomy of the basal ganglia in normal and Parkinsonian states. Neuroscience **76:** 335–343.
18. **Liu, Y., and R. H. Edwards.** 1997. The role of vesicular transport proteins in synaptic transmission and neural degeneration. Annu. Rev. Neurosci. **20:** 125–156.
19. **Liu, Y., D. Peter, A. Roghani, S. Schuldiner, G. G. Prive, D. Eisenberg, N. Brecha, and R. H. Edwards.** 1992. A cDNA that suppresses MPP^+ toxicity encodes a vesicular amine transporter. Cell **70:**539–551.
20. **Liu, Y., R. S. Erzurumlu, C. Chen, S. Jhaveri, and S. Tonegawa.** 1994. Whisker-related neuronal patterns fail to develop in the trigeminal brainstem nuclei of NMDAR1 knockout mice. Cell **76:**427–437.
21. **Mansour, S. L., K. R. Thomas, and M. R. Capecchi.** 1988. Disruption of the proto-oncogene int-2 in mouse embryo-derived stem cells: a general strategy for targeting mutations to non-selectable genes. Nature **336:**348–352.
22. **Melton, D. W., D. S. Konecki, J. Brennand, and C. T. Caskey.** 1984. Structure, expression, and mutation of the hypoxanthinephosphoribosyltransferase gene. Proc. Natl. Acad. Sci. USA **81:**2147–2151.
23. **Mittleman, G., H. J. Jones, and T. W. Robbins.** 1991. Sensitisation of amphetamine-stereotypy reduces plasma corticosterone: implications for stereotypy as a coping response. Behav. Neural Biol. **56:**170–182.
24. **Mohn, A. R., R. R. Gainetdinov, M. G. Caron, and B. H. Koller.** 1999. Mice with reduced NMDA receptor expression display behaviors related to schizophrenia. Cell **98:**427–436.
25. **Moore, R. Y., and F. E. Bloom.** 1979. Central catecholamine system: anatomy and physiology of norepinephrine and epinephrine systems. Annu. Rev. Neurosci. **2:**113–168.
26. **Nestler, E. J., and G. K. Aghajanian.** 1997. Molecular and cellular basis of addiction. Science **278:**58–63.
27. **Nieuwboer, A., W. De Weerdt, R. Dom, and E. Lesaffre.** 1998. A frequency and correlation analysis of motor deficits in Parkinson patients. Disabil. Rehabil. **20:**142–150.
28. **Peter, D., Y. Liu, C. Sternini, R. de Giorgio, N. Brecha, and R. H. Edwards.** 1995. Differential expression of two vesicular monoamine transporters. J. Neurosci. **15:** 6179–6188.
29. **Plagge, A., G. Kelsey, and N. D. Allen.** 1999. Directed mutagenesis in embryonic stem cells, p. 247–284. *In* I. J. Jackson and C. M. Abbott (ed.), Mouse genetics and transgenics. Oxford University Press, Oxford, United Kingdom.
30. **Robbins, T. W., G. Mittleman, J. O'Brien, and P. Winn.** 1990. The neuropsychological significance of stereotypy induced by stimulant drugs, p. 25–63. *In* S. J. Cooper and C. T. Dourish (eds.), Neurobiology of stereotyped behaviour. Oxford University Press, Claredon, United Kingdom.
31. **Schlomo, B.** 1997. The epidemiology of Parkinson's disease. Baillieres Text. Clin. Neurol. **6:**55–68.
32. **Seeman, P., C. Ulpian, C. Bergeron, P. Riederer, K. Jellinger, E. Gabriel, G. P. Reynolds, and W. W. Tourtellotte.** 1984. Bimodal distribution of dopamine receptor densities in brains of schizophrenics. Science **225:**728–731.
33. **Takahashi, N., and G. Uhl.** 1997. Murine vesicular monoamine transporter 2: molecular cloning and genomic structure. Mol. Brain Res. **49:**7–14.
34. **Takahashi, N., L. L. Miner, I. Sora, H. Ujike, R. S. Revay, V. Kostic, V. Jackson-Lewis, S. Przedborski, and G. R. Uhl.** 1997. VMAT2 knockout mice: heterozygotes display reduced amphetamine conditioned reward, enhanced amphetamine locomotion, and enhanced MPTP toxicity. Proc. Natl. Acad. Sci. USA **94:**9938–9943.
35. **Uhl, G. R.** 1998. Hypothesis: the role of dopaminergic transporters in selective vulnerability of cells in Parkinson's disease. Ann. Neurol. **43:**555–560.
36. **Wang, Y.-M., R. R. Gainetdinov, F. Fumagalli, F. Xu, S. R. Jones, C. B. Bock, G. W. Miller, R. M. Wightman, and M. G. Caron.** 1997. Knockout of the vesicular monoamine transporter 2 gene results in neonatal death and supersensitivity to cocaine and amphetamine. Neuron **19:**1285–1296.
37. **Young, W. S., T. I. Bonner, and M. R. Brann.** 1986. Mesencephalic dopamine neurons regulate the expression of neuropeptide mRNAs in the rat forebrain. Proc. Natl. Acad. Sci. USA **83:**9827–9831.